8th International Symposium on Magnetic Bearing
August 26-28, 2002, Mito, Japan

NONLINEAR ADAPTIVE CONTROL FOR A FLYWHEEL ROTOR-AMB SYSTEM WITH UNKNOWN PARAMETER

Selim Sivrioglu, Kenzo Nonami
Department of Electronics
and Mechanical Engineering
Chiba University, Chiba-Japan.
selim@mec2.tm.chiba-u.ac.jp

Atsushi Kubo, Ryouichi Takahata
Research and Development Center
Koyo Seiko Co. Ltd.
333 Toichi-cho,Kashihara
Nara 634-0008, Japan.

ABSTRACT

This study proposes a nonlinear adaptive output feedback type backstepping control for a zero power magnetic bearing system to achieve a better performance. Recently, integrator backstepping control has become popular in magnetic bearing control system design due to handling nonlinearities without any cancelation. On the other hand, the backstepping control is essentially a state-feedback control approach and requires full states of the control system. Since only the displacement of the rotor is measured in a magnetic bearing system, the numerical differentiation of the velocity from the displacement degrades the performance of the integrator backstepping controller in implementation. An alternative way for the controller design, nonlinear observers are introduced and unmeasured state is estimated using the observers. Moreover, the magnetic force coefficient is treated as unknown constant parameter and an adaptation procedure of the unknown parameter is formulated. The proposed control is experimentally verified for a flywheel magnetic bearing system and obtained good results.

INTRODUCTION

In recent years, development of high efficient and clean energy storage systems become an important research topic due to environmental problems. Flywheel energy storage systems which store rotating kinetic energy by high-speed rotation have promising future because of cleanliness and high-density energy storage. It is important for a flywheel system that windy loss and bearing loss of flywheel are reduced in order to keep electric power for several hours. One of the aims of this study is to investigate the applicability of the low power consumption active magnetic bearings to flywheel energy storage systems. Basically, an active magnetic bearing provides support of a rotor using electromagnetic forces without any mechanical contact. An online active control system is necessary to maintain the stability due to instability of the rotor-magnetic bearing in open-loop. Although a frictionless suspension is an advantage of the AMBs, the power consumption and energy loses may not reduced easily. In conventional AMB systems, a constant bias current is introduced into the coils of the AMB to obtain a linear model. A source of the losses in a magnetic bearing system is the bias current itself. Due to generating a constant magnetic field for the active control, the bias current leads to eddy current and rotational losses much larger than the nonlinear control. Moreover, the magnetic force coefficient is not truly identified and has likely a variation during control operation of the magnetic bearing. It is expected that a reliable adaptation of the magnetic force coefficient as a unknown parameter might increase control performance.

Nonlinear control of the active magnetic bearings has been previously studied using different approaches. In reference [1], a nonlinear control approach is proposed using differential flatness. As a control design, the nonlinear integrator backstepping control [2] has attracted much attention to solve control problems for active magnetic bearing applications [3]. In this study, a nonlinear control structure is defined for a single axis magnetic bearing and then a adaptive control design is presented using backstepping approach with experimental verifications.

NONLINEAR CONTROL STRUCTURE

The nonlinear control defined here is to switch the control current of the electromagnets of an active magnetic bearing according to the rotor position. As a difference from the linear control, no bias current is employed in the proposed nonlinear control. In an attractive type bearing configuration of a pair magnet shown in Figure 1, when the rotor approaches to one of the magnets, the coil current in the approached side magnet switched to zero while opposite side magnet has a current flow to generate attractive force. The switching process continues until the rotor is brought to the origin where the stability is provided. Since the

origin is zero axis for the rotor, the required power is theoretically zero if the rotor is suspended at the origin. If the coil current is assumed to be the control input, then the nonlinear equation of the rotor-active magnetic bearing system for a one degree-of-freedom shown in Figure 1 is derived as

$$M\ddot{x} = K\left[\frac{i_1^2}{(X_0 - x)^2} - \frac{i_2^2}{(X_0 + x)^2}\right] \tag{1}$$

where M and K are the mass of the rotor and the magnetic force coefficient, respectively. i_1 and i_2 are the control currents. X_0 denotes the air gap. The dynamics of the electrical part of the electromagnet is neglected because the coil current of the each electromagnet is assumed to be controlled by a high-bandwidth current loop. In most industrial use active magnetic bearing system, to drive the coil with such a current loop is common and eliminates the dependence of performance on the electromagnet coil resistance and inductance [4]. Using the variable transformation $x_1 = x$, $x_2 = \dot{x}$, the second order system is obtained as

$$\begin{aligned} \dot{x}_1 &= x_2 \\ \dot{x}_2 &= \begin{bmatrix} \theta\beta_1(x_1) & -\theta\beta_2(x_1) \end{bmatrix} \begin{bmatrix} u_1 \\ u_2 \end{bmatrix} \\ y &= x_1 \end{aligned} \tag{2}$$

where $u_1 = i_1^2$ and $u_2 = i_2^2$ are the control inputs. The output is represented by y. The unknown parameter θ and the nonlinear functions β_1 and β_2 are defined as

$$\theta = \frac{K}{M},\ \beta_1(x_1) = \frac{1}{(X_0 - x_1)^2},\ \beta_2(x_1) = \frac{1}{(X_0 + x_1)^2} \tag{3}$$

Note that the nonlinear functions β_1 and β_2 are strictly positive functions of the state x_1. It seems that the equation (2) has multi-input structure but in reality only one control input is effective at any time depending on the rotor position such as

$$\begin{aligned} \dot{x}_1 &= x_2 \\ \dot{x}_2 &= \theta\beta u \\ y &= x_1 \end{aligned}$$
$$\begin{array}{llll} x_1 \geq 0 & u = u_2, & u_1 = 0, & \beta = -\beta_2(x_1) \\ x_1 < 0 & u = u_1, & u_2 = 0, & \beta = \beta_1(x_1) \end{array} \tag{4}$$

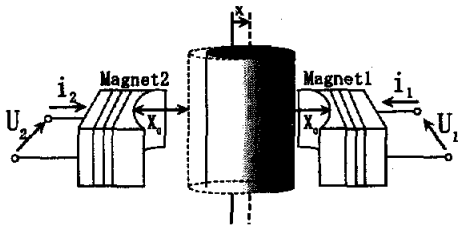

FIGURE 1: A single axis rotor-magnetic bearing

OBSERVER BACKSTEPPING

Nonlinear Observers

In practice, only the displacement of the rotor is measured, and the velocity is not available for the feedback. To estimate the unmeasured state x_2, an exponentially convergent observer is introduced into the control system such as

$$\hat{x}_2 = \xi + \theta\zeta + kx_1 \tag{5}$$

where ξ and ζ denote the states of the filters. Also, k is a positive parameter. The first filter is for the part of the plant that does not contain the unknown parameter θ and the second one is for the unknown part of the plant. The filters are defined as

$$\begin{aligned} \dot{\xi} &= -k\xi - k^2 x_1 \\ \dot{\zeta} &= -k\zeta + \beta(x_1)u \end{aligned} \tag{6}$$

If the initial conditions are $\xi(0) = 0$ and $\zeta(0) = 0$, then it is guaranteed that the estimation error ϵ exponentially converges to zero such as

$$\begin{aligned} \epsilon &= x_2 - \hat{x}_2 \\ \dot{\epsilon} &= \dot{x}_2 - \dot{\xi} - \theta\dot{\zeta} - k\dot{x}_1 \\ &= k(\xi + \theta\zeta + kx_1) - kx_2 \\ &= -k\epsilon \end{aligned} \tag{7}$$

Control Development

The control system structure given in the equation (4) falls into a class of nonlinear strict-feedback system and involves a nonlinear control system design approach such as backstepping. Basically, backstepping is a recursive control design approach which consider the some of state variables as virtual controls in every step of the design. In general, the objective of the control is to track the reference $y_r(t)$ with the system output $y(t)$. The tracking error is defined as

$$z_1 = y - y_r \tag{8}$$

The derivative of the z_1 is obtained as

$$\begin{aligned} \dot{z}_1 &= \dot{x}_1 - \dot{y}_r \\ &= x_2 - \dot{y}_r \end{aligned} \tag{9}$$

Since x_2 is not measured, the estimate of it will be used. Now substituting the equation (5) into (9), the derivative of z_1 becomes

$$\dot{z}_1 = \xi + \theta\zeta + kx_1 + \epsilon \tag{10}$$

Note that the reference input y_r is zero for the rotor magnetic bearing system. In the equation (10), the only variable that contains control input u is the variable ζ. Thus it may be used as virtual control for the second error variable such as

$$z_2 = \zeta - \alpha_1 \tag{11}$$

The stabilizing function α_1 is chosen as

$$\alpha_1 = \hat{\rho}(-c_1 z_1 - d_1 z_1 - k x_1 - \xi) = \hat{\rho}\bar{\alpha}_1 \tag{12}$$

where $c_1 > 0$, $d_1 > 0$. Note that to eliminate the variable ζ in the equation (10), the stabilizing function α_1 is multiplied by $\hat{\rho}$ which is an estimate of the parameter $\rho = 1/\theta$. Moreover, as a difference from the integrator backstepping procedure, d_1 is added to counteract the estimation error ϵ. Now, the derivative of z_1 becomes

$$\begin{aligned}\dot{z}_1 &= \xi + \theta(z_2 + \alpha_1) + k x_1 + \epsilon \\ &= \xi + \theta(z_2 + \hat{\rho}\bar{\alpha}_1) + k x_1 + \epsilon \\ &= \xi + \theta[z_2 + (\rho - \tilde{\rho})\bar{\alpha}_1] + k x_1 + \epsilon \\ &= \theta z_2 - c_1 z_1 - d_1 z_1 - \theta\tilde{\rho}\bar{\alpha}_1 + \epsilon\end{aligned} \tag{13}$$

where $\hat{\rho} = \rho - \tilde{\rho}$. Here $\tilde{\rho}$ denotes the error in the estimation of $\hat{\rho}$. For the first error variable, a candidate of Lyapunov function is defined as

$$V_1 = \frac{1}{2}z_1^2 + \frac{1}{2\gamma}\theta(\rho - \hat{\rho})^2 + \frac{1}{2kd_1}\epsilon^2 \tag{14}$$

where γ is the adaptation gain. The derivative of V_1 is obtained as

$$\begin{aligned}\dot{V}_1 &= z_1\dot{z}_1 - \frac{1}{\gamma}\theta(\rho - \hat{\rho})\dot{\hat{\rho}} + \frac{1}{kd_1}\epsilon\dot{\epsilon} \\ &= \theta z_1 z_2 - c_1 z_1^2 - \theta(\rho - \hat{\rho})(\bar{\alpha}_1 z_1 + \frac{1}{\gamma}\dot{\hat{\rho}}) \\ &\quad \underbrace{- d_1\left(z_1 - \frac{1}{2d_1}\epsilon\right)^2 + \frac{1}{4d_1}\epsilon^2}_{-d_1 z_1^2 + z_1\epsilon} - \frac{1}{d_1}\epsilon^2 \\ &\leq \theta z_1 z_2 - c_1 z_1^2 - \theta(\rho - \hat{\rho})(\bar{\alpha}_1 z_1 + \frac{1}{\gamma}\dot{\hat{\rho}}) - \frac{3}{4d_1}\epsilon^2\end{aligned} \tag{15}$$

The $\theta(\rho - \hat{\rho})$ term in the above inequality can be eliminated using the update law as follows:

$$\dot{\hat{\rho}} = -\gamma\bar{\alpha}_1 z_1 \tag{16}$$

Since the term $\theta z_1 z_2$ remained in (15) , a global stability condition is not satisfied in this step. The second step is to expend the control design to include the error variable z_2. For this aim, the derivative of the second error variable is obtained as

$$\dot{z}_2 = \dot{\zeta} - \dot{\alpha}_1 \tag{17}$$

Here, the stabilizing function α_1 is a function of y, ξ and $\hat{\rho}$, therefore, the derivative α_1 is obtained as

$$\dot{\alpha}_1 = \frac{\partial\alpha_1}{\partial y}\dot{y} + \frac{\partial\alpha_1}{\partial\xi}\dot{\xi} + \frac{\partial\alpha_1}{\partial\hat{\rho}}\dot{\hat{\rho}} \tag{18}$$

Substituting the equations (6) and (18) into the equation (17), the derivative of z_2 becomes

$$\begin{aligned}\dot{z}_2 = &-k\zeta + \beta(x_1)u - \frac{\partial\alpha_1}{\partial y}(\xi + \theta\zeta + k x_1 + \epsilon) \\ &- \frac{\partial\alpha_1}{\partial\xi}(-k\xi + k^2 x_1) - \frac{\partial\alpha_1}{\partial\hat{\rho}}\dot{\hat{\rho}}\end{aligned} \tag{19}$$

The equation (19) is not desired form because the unknown parameter θ appears. Moreover, the disturbance ϵ is multiplied by the nonlinear term $\frac{\partial\alpha_1}{\partial y}$. To employ nonlinear damping and to eliminate the unknown parameter, the equation (19) is equalized as follows:

$$\begin{aligned}&-c_2 z_2 - \hat{\theta} z_1 - d_2\left(\frac{\partial\alpha_1}{\partial y}\right)^2 z_2 - \frac{\partial\alpha_1}{\partial y}\epsilon - \frac{\partial\alpha_1}{\partial y}\tilde{\theta}\zeta = \\ &-k\zeta + \beta(x_1)u - \frac{\partial\alpha_1}{\partial y}(\xi + \theta\zeta + k x_1 + \epsilon) \\ &- \frac{\partial\alpha_1}{\partial\xi}(-k\xi - k^2 x_1) - \frac{\partial\alpha_1}{\partial\hat{\rho}}\dot{\hat{\rho}}\end{aligned} \tag{20}$$

where $\hat{\theta}$ is the estimate of the unknown parameter θ. Also, $\tilde{\theta}$ represents error in this estimation. From the equation (20), the control input u is chosen as

$$\begin{aligned}u = \frac{1}{\beta(x_1)}\Bigg[&-c_2 z_2 - d_2\left(\frac{\partial\alpha_1}{\partial y}\right)^2 z_2 - \hat{\theta} z_1 + k\zeta \\ &+ \frac{\partial\alpha_1}{\partial y}(\xi + \hat{\theta}\zeta + k x_1) + \frac{\partial\alpha_1}{\partial\xi}(-k\xi - k^2 x_1) + \frac{\partial\alpha_1}{\partial\hat{\rho}}\dot{\hat{\rho}}\Bigg]\end{aligned} \tag{21}$$

Substituting (21) into the (19), the derivative of z_2 becomes

$$\dot{z}_2 = -c_2 z_2 - d_2\left(\frac{\partial\alpha_1}{\partial y}\right)^2 z_2 - (\theta - \tilde{\theta})z_1 - \frac{\partial\alpha_1}{\partial y}\tilde{\theta}\zeta - \frac{\partial\alpha_1}{\partial y}\epsilon \tag{22}$$

The Lyapunov function is augmented for the second error variable z_2 as follows

$$V_2 = V_1 + \frac{1}{2}z_2^2 + \frac{1}{2\gamma}(\theta - \hat{\theta})^2 + \frac{1}{2kd_2}\epsilon^2 \tag{23}$$

The derivative of V_2 is derived as

$$\begin{aligned}\dot{V}_2 &= \dot{V}_1 + z_2\dot{z}_2 - \frac{1}{\gamma}(\theta - \hat{\theta})\dot{\hat{\theta}} + \frac{1}{kd_2}\epsilon\dot{\epsilon} \\ &= -c_1 z_1^2 - c_2 z_2^2 \underbrace{- d_2\left(\frac{\partial\alpha_1}{\partial y}z_2 - \frac{1}{2d_2}\epsilon\right)^2 + \frac{1}{4d_2}\epsilon^2}_{d_2(\frac{\partial\alpha_1}{\partial y})^2 z_2^2 - \frac{\partial\alpha_1}{\partial y}\epsilon z_2} \\ &\quad - \frac{1}{d_2}\epsilon^2 - \frac{3}{4d_1}\epsilon^2 \\ &\leq -c_1 z_1^2 - c_2 z_2^2 + (\theta - \hat{\theta})\left(z_1 z_2 - \frac{\partial\alpha_1}{\partial y}\zeta z_2 - \frac{1}{\gamma}\dot{\hat{\theta}}\right) \\ &\quad - \left(\frac{3}{4d_1} + \frac{3}{4d_2}\right)\epsilon^2\end{aligned} \tag{24}$$

where $c_2 > 0, d_2 > 0$. The unknown part of $(\theta - \hat{\theta})$ in the equation (24) is eliminated using the update law

$$\dot{\hat{\theta}} = \gamma\left(z_1 z_2 - \frac{\partial\alpha_1}{\partial y}\zeta z_2\right) \tag{25}$$

It is clear that a global stability is maintained in the final Lyapunov function. Now, the control currents i_1 and i_2 can be computed from the control input u obtained in the equation (21).

FLYWHEEL ROTOR-AMB SYSTEM

A vertically designed five axis controlled active magnetic bearing system shown in Figure 2(a) is used for modeling, simulations and experiments. The AMB system which is manufactured by Koyo Seiko Corporation Ltd., Japan, is consists of a main AMB spindle, a control unit and a high-frequency inverter. The parameters of the rotor-AMB system are given in Table 1. A separate test system which is placed in a vacuum chamber by mounting an 8 kg CFRP flywheel to an identical AMB system is also available for rotational experiments. In this study, the rotational tests are realized using the test system given Figure 2(a).

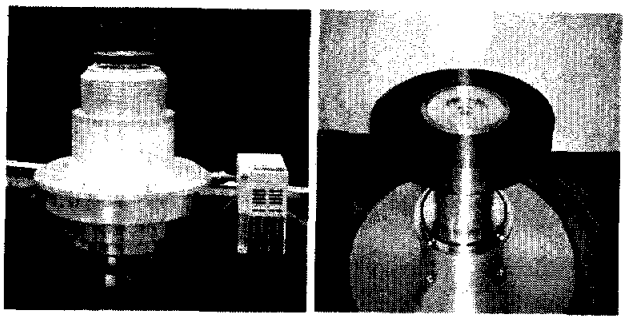

(a) (b)

FIGURE 2: The rotor-AMB system
(a) without flywheel (b) with flywheel

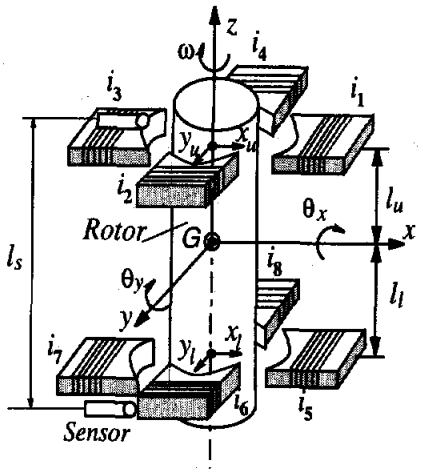

FIGURE 3: Rotor-AMB system

TABLE 1: Parameters of the rotor-AMB system

Symbol	Value	Unit
M	4.85	kg
I_r	2.90×10^{-2}	kgm^2
I_a	2.22×10^{-2}	kgm^2
l_u	4.166×10^{-2}	m
l_l	7.602×10^{-2}	m
l_s	16.28×10^{-2}	m
K_u	4.47×10^{-6}	Nm^2/A^2
K_l	3.10×10^{-5}	Nm^2/A^2
X_0, Y_0	0.25×10^{-3}	m

Model of the Rotor-AMB System

It is supposed that axial and radial directions are separated and the dynamics of the rotor may be investigated independently in both directions. Since axial direction is controlled with a PID controller, only the radial directions will be modeled for a control design. Note that only the rigid modes are considered due to small size of the rotor. The equation of motion of the rigid rotor-active magnetic bearing system depicted in Figure 3 is derived as

$$\begin{aligned} M\ddot{x}_g &= (F_1 - F_3) + (F_5 - F_7) \\ I_r\ddot{\theta}_y &= (F_1 - F_3)l_u - (F_5 - F_7)l_l \\ M\ddot{y}_g &= (F_2 - F_4) + (F_6 - F_8) \\ I_r\ddot{\theta}_x &= -(F_2 - F_4)l_u + (F_6 - F_8)l_l \end{aligned} \tag{26}$$

where x_g and y_g denote the displacement of the rotor's center of mass. Similarly, θ_y and θ_x are the angular displacement of the rotor around x and y axes. F_1, F_2, F_3, and F_4 denote the electromagnetic forces for the upper bearing in x and y directions. Similarly, F_5, F_6, F_7, and F_8 show the electromagnetic forces for the lower bearing. For x direction, the upper and lower bearing forces are given as

$$\begin{aligned} F_1 &= \frac{K_u i_1^2}{(X_0 - x_u)^2}, & F_3 &= \frac{K_u i_3^2}{(X_0 + x_u)^2} \\ F_5 &= \frac{K_l i_5^2}{(X_0 - x_l)^2}, & F_7 &= \frac{K_l i_7^2}{(X_0 + x_l)^2} \end{aligned} \tag{27}$$

The electromagnetic forces have the same structure with different indices for the lower and upper bearings in y direction.

Collocated System Transformations

The equations of motion obtained in (26) are derived according to the movement of the rotor's center of mass. On the other hand, the measured signals are the displacements of the rotor at the lower and upper sensor locations. In the above rotor-AMB system, four position sensors are located near to the upper and lower actuators. Since sensor locations are distinct from the mass center, the computation of the displacements of the rotor's center of mass and angular displacements are necessary during control operation. In this study, it is aimed to form a direct correlation between measured outputs and control inputs. Instead of computing the displacements x_g, y_g, θ_y and θ_x, the computation of the displacements of the rotor at the magnet locations makes the control system collocated. For this aim, dynamics of the rotor may be transformed to the actuator locations as follows:

$$\begin{aligned} x_u &= x_g + l_u\theta_y, & y_u &= y_g - l_u\theta_x \\ x_l &= x_g - l_l\theta_y, & y_l &= y_g + l_l\theta_x \end{aligned} \tag{28}$$

where x_u and x_l show the displacements of the rotor at the upper and lower actuator locations in x direction,

respectively. Similarly, y_u and y_l denote the displacements at the actuator locations in y direction. Taking the double derivative of the above equations and substituting the equation (26) and (27) into the obtained derivations, the collocated system equations are derived as

$$\begin{aligned}
\ddot{x}_u &= a_u K_u \left[\frac{i_1^2}{(X_0 - x_u)^2} - \frac{i_3^2}{(X_0 + x_u)^2} \right] \\
\ddot{x}_l &= a_l K_l \left[\frac{i_5^2}{(X_0 - x_l)^2} - \frac{i_7^2}{(X_0 + x_l)^2} \right] \\
\ddot{y}_u &= a_u K_u \left[\frac{i_2^2}{(Y_0 - y_u)^2} - \frac{i_4^2}{(Y_0 + y_u)^2} \right] \\
\ddot{y}_l &= a_l K_l \left[\frac{i_6^2}{(Y_0 - y_l)^2} - \frac{i_8^2}{(Y_0 + y_l)^2} \right]
\end{aligned} \tag{29}$$

where

$$a_u = \left(\frac{1}{M} + \frac{l_u^2}{I_r} \right) \qquad a_l = \left(\frac{1}{M} + \frac{l_l^2}{I_r} \right) \tag{30}$$

The state-space model of the control system is obtained as

$$\begin{bmatrix} \dot{X}_1 \\ \dot{X}_2 \end{bmatrix} = \begin{bmatrix} 0 & I \\ 0 & 0 \end{bmatrix} \begin{bmatrix} X_1 \\ X_2 \end{bmatrix} + \Theta \begin{bmatrix} 0_{4\times 8} \\ \beta(X_1) \end{bmatrix} U \tag{31}$$

where

$$\begin{aligned}
X_1^T &= \begin{bmatrix} x_u & x_l & y_u & y_l \end{bmatrix}^T \\
X_2^T &= \begin{bmatrix} \dot{x}_u & \dot{x}_l & \dot{y}_u & \dot{y}_l \end{bmatrix}^T \\
U^T &= \begin{bmatrix} u_1 & u_3 & u_5 & u_7 & u_2 & u_4 & u_6 & u_8 \end{bmatrix}^T
\end{aligned} \tag{32}$$

Controller Design

Since the equations (29) are independent of each other, the controller design can be done separately using these equations. The design procedure is completely same as defined in previous section.

CONTROL VERIFICATIONS

Simulations

The simulation results are obtained using the state-space model obtained in (31). Figure 4 shows the response of the rotor for a 0.1 mm initial step reference input. The rotor is perfectly brought to the origin by the nonlinear adaptive control. The control currents are shown in Figure 5 for the same step reference input. Since simulation is representing an ideal case, the control currents converges to zero after the rotor suspended at the origin. The value of the control Lyapunov function and estimation error converges to zero as shown in Figure 6. The estimated parameters $\hat{\rho}$ and $\hat{\theta}$ are also shown in Figure 7.

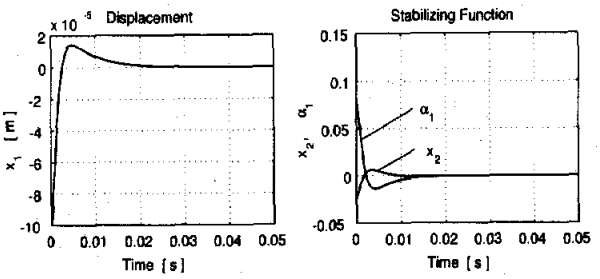

FIGURE 4: Step reference response

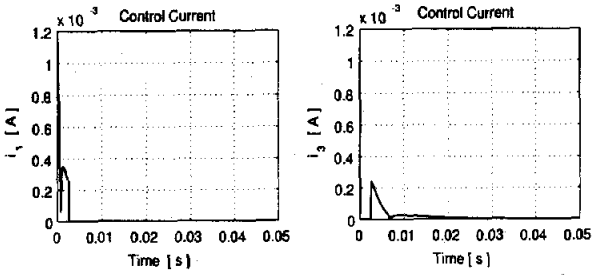

FIGURE 5: Control currents

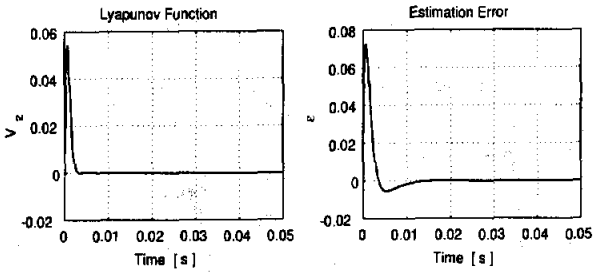

FIGURE 6: Lyapunov function and estimation error

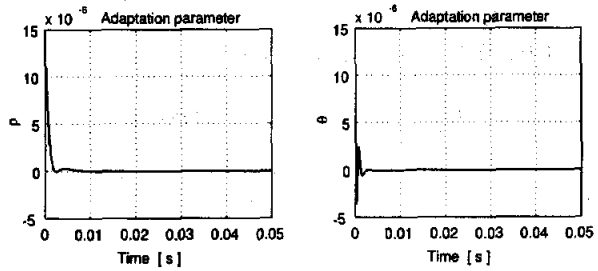

FIGURE 7: Estimated parameters

Experiments

A feedback control system is established with a digital signal processor(TMS320C40) to realize experiments. The control system is a multi-input multi-output structure with four displacements measured by four eddy-current position sensors and eight computed control current signals for actuators. The control inputs are supplied to electromagnets through D/A converters and power amplifiers. For non-rotating condition of the rotor, the transient response of the control system and the convergence of the adaptive controller are shown in Figures 8-9. The experimental results incline the simulations in general. The control currents for the upper bearing in the x direction is shown in

Figure 10 for levitation case. Note that the control currents are multiplied by an amplifying factor such as $K_f = 1500$ since the control currents obtained in simulations(Figure 5) is quite small to levitate the rotor. Rotor dynamics at critical speeds has considerable effect on the control currents as shown in Figure 11. At higher rotational frequencies, the rotor is balanced with imbalance forces and only one electromagnet has current flow as seen in Figure 12. The locus of the rotor for different rotational frequencies are presented in Figure 13.

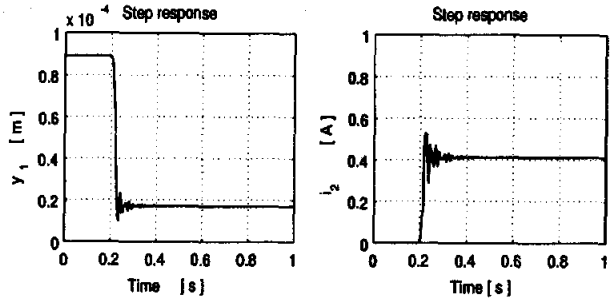

FIGURE 8: Step response

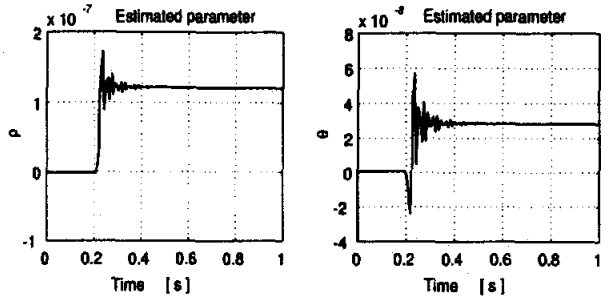

FIGURE 9: Online parameter estimation

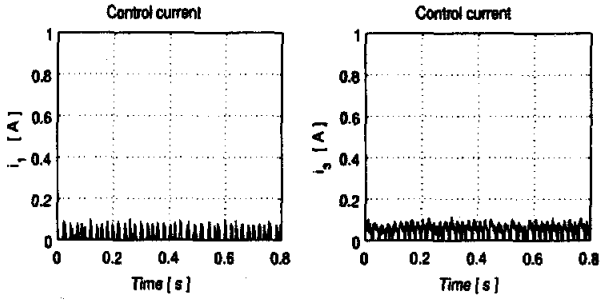

FIGURE 10: Control currents ($\omega = 0$)

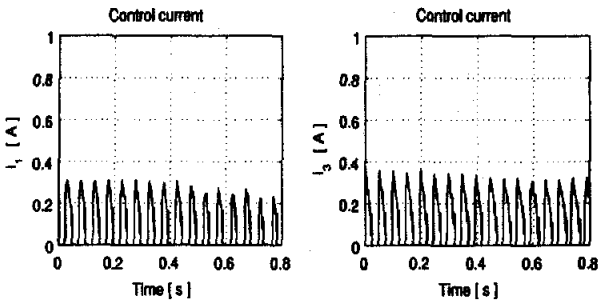

FIGURE 11: Control currents ($\omega = 20$ Hz)

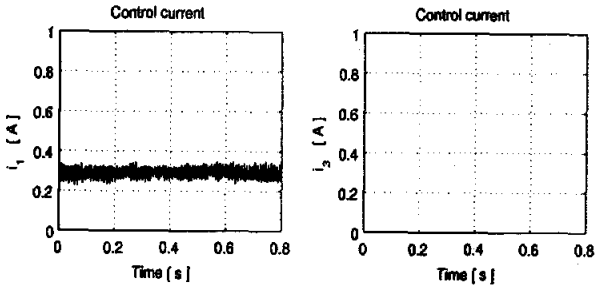

FIGURE 12: Control currents ($\omega = 100$ Hz)

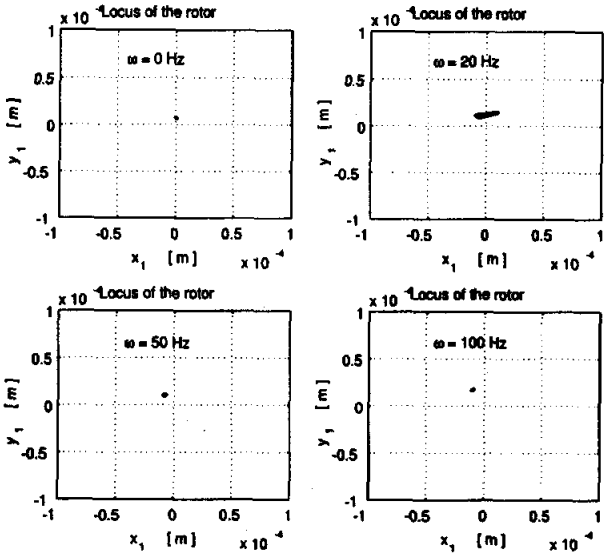

FIGURE 13: Locus of the rotor

CONCLUSIONS

In this study, a low energy consumption AMB system is realized using a nonlinear adaptive control approach. One of the important properties of the proposed control is the complete on-off structure of the control currents. While one side of the pair magnet has a current flow, the other side has always no current flow anymore. The on-off structure of the control has no deteriorating effects on the stability of the control system.

References

[1] J. Levine, J. Lottin, J-C. Ponsart: A Nonlinear Approach to the Control of Magnetic Bearing, IEEE Trans. on Control System Technology, Vol.4, No.5, pp. 524-544, 1996.

[2] M. Krstic, I. Kanellakopoulos, P. Kokotovic, *Nonlinear and Adaptive Control Design*, John W.& Sons, Inc., 1995.

[3] M.S. Queiroz, D.M. Dawson, *Nonlinear Control of Active Magnetic Bearings: A Backstepping Appproach*, IEEE Trans. on Control System Technology, Vol.4, No.5, pp. 545-552, 1996.

[4] D.L. Trumper, S.M. Olson, P.K. Subrahmanyan, *Linearizing Control of Magnetic Suspension System*, IEEE Transactions on Control System Technology, Vol.5, No.4, pp. 427-437, 1997.